

Investigation of a universal behavior between Néel temperature and staggered magnetization density for a three-dimensional quantum antiferromagnet

M.T. Kao and F.J. Jiang^a

Department of Physics, National Taiwan Normal University, 88, Sec.4, Ting-Chou Rd., 116 Taipei, Taiwan

Received 1 August 2013 / Received in final form 5 September 2013
Published online (Inserted Later) – © EDP Sciences, Società Italiana di Fisica, Springer-Verlag 2013

Abstract. We simulate the three-dimensional quantum Heisenberg model with a spatially anisotropic ladder pattern using the first principles Monte Carlo method. Our motivation is to investigate quantitatively the newly established universal relation $T_N/\sqrt{c^3} \propto \mathcal{M}_s$ near the quantum critical point (QCP) associated with dimerization. Here T_N , c , and \mathcal{M}_s are the Néel temperature, the spinwave velocity, and the staggered magnetization density, respectively. For all the physical quantities considered here, such as T_N and \mathcal{M}_s , our Monte Carlo results agree nicely with the corresponding results determined by the series expansion method. In addition, we find it is likely that the effect of a logarithmic correction, which should be present in $(3+1)$ -dimensions, to the relation $T_N/\sqrt{c^3} \propto \mathcal{M}_s$ near the investigated QCP only sets in significantly in the region with strong spatial anisotropy.

1 Introduction

While being the simplest models, Heisenberg-type models provide qualitatively, or even quantitatively useful information regarding the properties of cuprate materials. For example, the spatially anisotropic quantum Heisenberg model on the square lattice with different antiferromagnetic couplings in the 1 and 2 directions is demonstrated to be relevant for the underdoped cuprate superconductor $\text{YBa}_2\text{Cu}_3\text{O}_{6.45}$ [1,2]. Specifically, it is argued that this model provides a possible mechanism for the newly discovered pinning effects of the electronic liquid crystal in $\text{YBa}_2\text{Cu}_3\text{O}_{6.45}$ [3]. Because of their phenomenological importance, these models continue to attract a lot of attention analytically and numerically. In addition to being relevant to real materials, Heisenberg-type models on geometrically nonfrustrated lattices are important from a theoretical point of view as well. This is because these models can be simulated very efficiently using first principles Monte Carlo methods. Hence they are very useful in exploring ideas and examining theoretical predictions [4–12].

Recently a new universal behavior between the thermal and quantum properties of $(3+1)$ -dimensional dimerized quantum antiferromagnets has been established [13,14]. Specifically, using the relevant field theory, it is shown that the Néel temperature T_N can be related to the staggered magnetization density \mathcal{M}_s near a quantum critical point (QCP). This new universal property is then compared with experimental data for TlCuCl_3 in reference [15] and the agreement is impressive. In addition, in reference [14]

the relevant series expansion calculations are performed for the $(3+1)$ -dimensional ladder-dimer quantum antiferromagnet. The obtained results match reasonably well with the corresponding field theory predictions. Similar behavior was obtained in Monte Carlo simulations of [16] with various kinds of model.

Motivated by this newly established universal relation between thermal and quantum properties close to a QCP as well as to study this scaling behavior quantitatively, we simulate the $(3+1)$ -dimensional ladder-dimer quantum Heisenberg model using the first principles Monte Carlo method. The relevant quantities such as T_N , \mathcal{M}_s , and the spinwave velocity c are determined with high precision. We find that our results agree nicely with the series expansion calculations presented in reference [14]. In particular, with an empirical fitting ansatz, our Monte Carlo data imply that the effect of a logarithmic correction, which should be present in $(3+1)$ -dimensions, to the relation $T_N/\sqrt{c^3} \propto \mathcal{M}_s$ near the considered QCP only sets in significantly in the region with strong spatial anisotropy.

2 Microscopic model and corresponding observables

The three-dimensional quantum Heisenberg model considered in this study is defined by the Hamilton operator

$$H = \sum_{\langle xy \rangle} J \vec{S}_x \cdot \vec{S}_y + \sum_{\langle x'y' \rangle} J' \vec{S}_{x'} \cdot \vec{S}_{y'}, \quad (1)$$

^a e-mail: fjjiang@ntnu.edu.tw

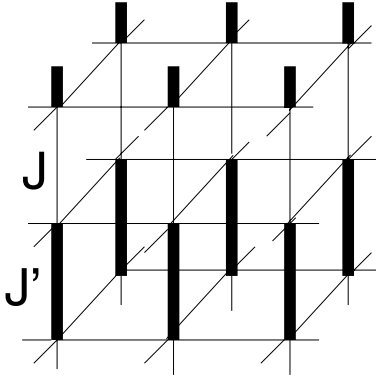


Fig. 1. The (3+1)-dimensional spatially anisotropic quantum Heisenberg model considered in this study.

where J (J') is the antiferromagnetic exchange coupling connecting nearest neighbor spins $\langle xy \rangle$ ($\langle x'y' \rangle$). The model described by equation (1) and studied here is illustrated in Figure 1. To investigate the newly established universal behavior between T_N and \mathcal{M}_s near the critical point induced by dimerization, the spin stiffnesses in all spatial directions, which are defined by

$$\rho_{si} = \frac{1}{\beta L_1 L_2 L_3} \langle W_i^2 \rangle, \quad (2)$$

are measured in our simulations. Here β is the inverse temperature, L_i refers to the spatial box size in the i direction, and $\langle W_i^2 \rangle$ with $i \in \{1, 2, 3\}$ is the winding number squared in the i direction. In addition, the observable $\langle (m_s^z)^2 \rangle$ is recorded in our calculations as well in order to determine \mathcal{M}_s . Here m_s^z is the z component of the staggered magnetization $\vec{m}_s = \frac{1}{L_1 L_2 L_3} \sum_x (-1)^{x_1+x_2+x_3} \vec{S}_x$. To perform the investigation, using the stochastic series expansion algorithm (SSE) with operator-loop update [17], we have carried out large scale Monte Carlo simulations with various inverse temperatures and box sizes L at several values of J'/J (we use $L_1 = L_2 = L_3$ in most of our simulations and J is set to be 1.0 throughout the calculations). Notice that, since the established QCP induced by dimerization is at $(J'/J)_c \sim 4.0$ [18], we have performed our calculations for $2.5 \leq J'/J \leq 4.0$. First of all, let us focus on our results of determining T_N .

3 Determination of the Néel temperatures

To calculate the Néel temperatures T_N for which the long-range antiferromagnetic order is destroyed for $T > T_N$, at each fixed $J'/J = 2.5, 3.0, 3.25, 3.375, 3.5, 3.625, 3.75$, and 3.875 , we have performed simulations by varying T for $L = 8, 12, 16, \dots, 36, 40$. Further, the numerical values of T_N are obtained by employing the standard finite-size scaling analysis to the relevant observables. Specifically, near T_N and for the observables $\rho_{si}L$ with $i \in \{1, 2, 3\}$, the curves of different L as a function of T should tend to intersect at T_N . Interestingly, we find that at each considered J'/J the correction to scaling for these observables

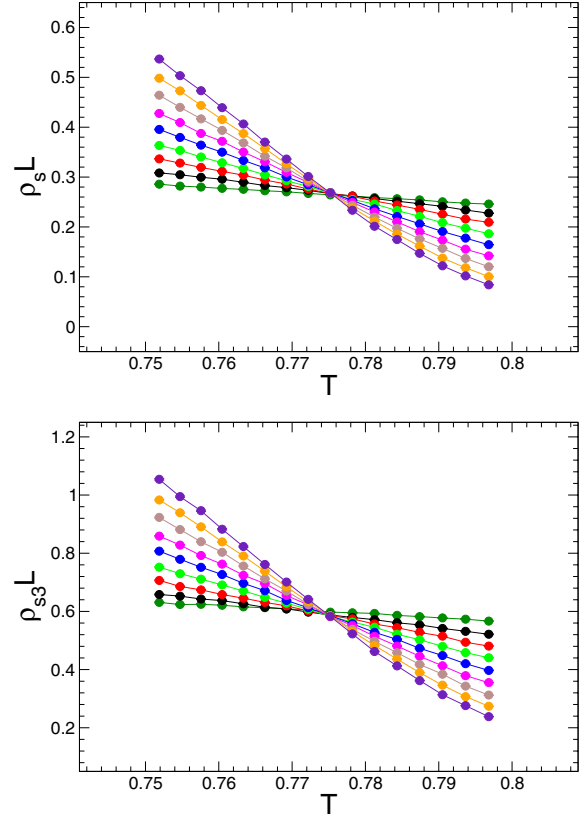


Fig. 2. Monte Carlo data of $\rho_s L$ (top panel) and $\rho_{s3} L$ (bottom panel) for $J'/J = 3.5$. The lines are added to guide the eye. The box sizes L for the data points on both panels are $L = 8, 12, 16, \dots, 32, 36$, and 40 .

is negligible when the relevant data points with $L \geq 20$ are employed in the analysis. In other words, our data can be described well by the expected leading scaling ansatz. Specifically, the ansatz employed in our finite-size scaling analysis is of the form $g(x)$, where g is a smooth function of the parameter x and x contains a factor linear in $(T - T_N)/T_N$. Indeed, by applying the fourth order Taylor expansion of the expected leading scaling ansatz to $\rho_s L = (\rho_{s1} + \rho_{s2})L/2$, we arrive at $T_N = 0.7751(2)$ for $J'/J = 3.5$ (top panel of Fig. 2). Using a third order Taylor expansion of the leading scaling form leads to a value of T_N which agrees nicely with $T_N = 0.7751(2)$. Employing the same procedure, the value of T_N determined from $\rho_{s3} L$ for $J'/J = 3.5$ is given by $0.7750(2)$ (bottom panel of Fig. 2). Notice that the T_N obtained from these two different observables agree with each other quantitatively. The T_N at other couplings J'/J are calculated with the same strategy and Table 1 summarizes our results of determining the values of T_N at the considered couplings J'/J . Notice a bootstrap resampling method is employed in obtaining the results in Table 1. In particular, the quoted errors are determined by a conservative estimate based on the standard deviations of the fits with good quality. Later these determined T_N will be used in examining the universal behavior between T_N and \mathcal{M}_s near the QCP associated with dimerization.

Table 1. The numerical values of T_N at $J'/J = 2.5, 3.0, 3.25, 3.375, 3.5, 3.625, 3.75, 3.875$ determined by applying the leading scaling ansatz to the relevant observables. All the χ^2/DOF of these fits are smaller than 1.6.

Observable	J'/J	T_N	J'/J	T_N
$\rho_s L$	2.5	1.0014(2)	3.5	0.7751(2)
$\rho_{s3} L$	2.5	1.0014(2)	3.5	0.7750(2)
$\rho_s L$	3.0	0.9317(2)	3.625	0.7087(3)
$\rho_{s3} L$	3.0	0.9316(2)	3.625	0.7086(3)
$\rho_s L$	3.25	0.8690(2)	3.75	0.6197(2)
$\rho_{s3} L$	3.25	0.8689(2)	3.75	0.6193(3)
$\rho_s L$	3.375	0.8270(2)	3.875	0.4853(3)
$\rho_{s3} L$	3.375	0.8269(2)	3.875	0.4849(4)

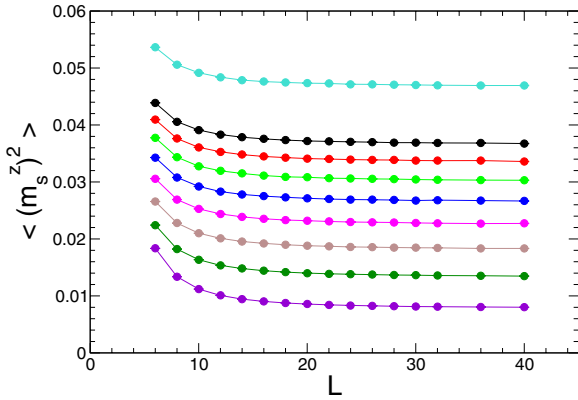


Fig. 3. Monte Carlo data of $\langle (m_s^z)^2 \rangle$ as functions of L . From top to bottom the corresponding values of J'/J for these curves are 2.5, 3.0, 3.125, 3.25, \dots , 3.75, and 3.875, respectively. The lines are added to guide the eye.

4 Determination of the staggered magnetization density

To calculate \mathcal{M}_s , we have measured the observable $\langle (m_s^z)^2 \rangle$. Specifically, by extrapolating the zero-temperature $\langle (m_s^z)^2 \rangle$ at finite lattice size to the bulk value $(m_s^z)^2(\infty)$, \mathcal{M}_s can then be obtained from $\mathcal{M}_s = \sqrt{3(m_s^z)^2(\infty)}$. Notice that to determine \mathcal{M}_s by this method one needs the zero-temperature values of $\langle (m_s^z)^2 \rangle$. We have carried out trial runs for $L = 20$ with $\beta J = 20$ and $\beta J = 40$ at $J'/J = 2.5, 3.0, 3.125, 3.25, 3.375, 3.5, 3.625, 3.75, 3.875$. The obtained values of $\langle (m_s^z)^2 \rangle$ for these two different inverse temperatures β at all the considered couplings J'/J agree reasonably well. Hence the extrapolation using the data of $\langle (m_s^z)^2 \rangle$ calculated with $\beta J = L$ in the simulations should lead to correct results. Indeed it has been demonstrated in reference [16] that the extrapolated values of $\langle (m_s^z)^2 \rangle$ for various couplings J'/J , determined with the data obtained from simulations employing $\beta J = L$ and $\beta J = 2L$, are consistent with each other. Figure 3 shows our $\langle (m_s^z)^2 \rangle$ data for $L = 6, 8, 10, \dots, 32, 36, 40$ at the considered J'/J . The extrapolation results for these data using the ansatz $a + b/L + c/L^2 + d/L^3$ are depicted

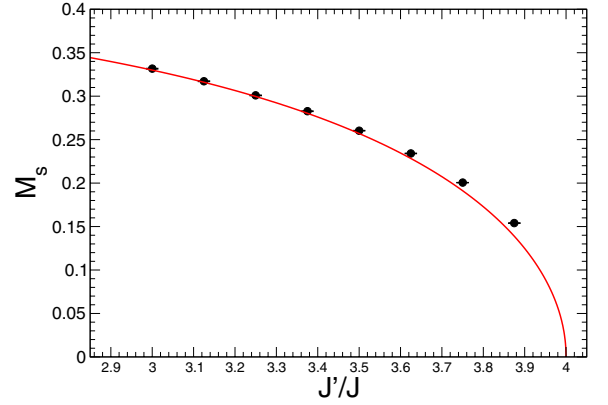


Fig. 4. Monte Carlo determination of \mathcal{M}_s as a function of J'/J . The solid curve is reproduced from reference [14] and is the fitting result based on series expansion calculations.

in Figure 4. In Figure 4 the solid curve is reproduced from reference [14] and is the fitting result based on series expansion calculations. The agreement between our Monte Carlo data and series expansion results of \mathcal{M}_s is remarkable.

5 Determination of the spinwave velocity

There are several methods to determine the low-energy constant c . Here we use the idea of winding numbers squared. Specifically, for each J'/J we adjust the ratio of L_1/L_3 so that all three spatial winding numbers squared take approximately the same values. Then we tune β in order to reach the condition $\langle W_t^2 \rangle \sim \langle W_i^2 \rangle$ for $i \in \{1, 2, 3\}$. Here $\langle W_t^2 \rangle$ is the temporal winding number squared. Once this condition is met, the numerical value of c is estimated to be $L/\beta_2 \leq c \leq L/\beta_1$, where $L = (L_1 L_2 L_3)^{1/3}$ and β_1 (β_2) stands for the largest (smallest) inverse temperature so that the criterion $\langle W_i^2 \rangle \leq \langle W_t^2 \rangle$ ($\langle W_i^2 \rangle \geq \langle W_t^2 \rangle$) for $i \in \{1, 2, 3\}$ is satisfied. For the isotropic case $J'/J = 1.0$, the spinwave theory predicts $c \sim 1.9091J$ [19]. Remarkably, for a trial simulation with $J'/J = 1.0$, $L_1 = L_2 = L_3 = 20$ and $\beta J = 10.476$ (hence $L/\beta \sim 1.9091J$), the ratio of the average of three spatial winding numbers squared and the temporal winding number squared is 0.994 approximately. This confirms the validity of calculating c using the idea of winding numbers squared. For each coupling J'/J studied here, we further consider at least two sets of box sizes for which the condition $\langle W_t^2 \rangle \sim \langle W_i^2 \rangle$ for $i \in \{1, 2, 3\}$ is satisfied. With this strategy, the numerical values of c obtained for $J'/J = 2.5, 3.0, 3.25, 3.5, 3.375, 3.625, 3.75, 3.875$, and 4.0 are shown in Table 2. The results shown in Table 2 imply that the values of c at the considered couplings are already convergent to the corresponding bulk values. Even if some of our determined c have not reached their bulk values, one expects the deviations to be very small. Hence such systematic uncertainty would have little impact on our investigation of the universal relation between T_N and \mathcal{M}_s .

Table 2. The numerical values of c obtained through the winding numbers squared for various couplings J'/J .

J'/J	L_1	L_3	c/J	J'/J	L_1	L_3	c/J
2.5	22	28	2.215(8)	3.5	46	62	2.348(10)
2.5	36	46	2.215(9)	3.625	22	30	2.360(12)
3.0	32	42	2.282(13)	3.625	34	46	2.360(13)
3.0	44	58	2.283(11)	3.75	22	30	2.376(12)
3.25	12	16	2.317(7)	3.75	44	60	2.378(11)
3.25	18	24	2.317(8)	3.875	16	22	2.391(7)
3.25	24	32	2.317(11)	3.875	32	44	2.389(8)
3.375	12	16	2.335(12)	4.0	16	22	2.408(13)
3.375	24	32	2.334(13)	4.0	32	44	2.405(15)
3.5	34	46	2.347(12)	4.0	42	58	2.401(10)

6 Comparison between theoretical predictions and Monte Carlo results

In reference [14] the following universal relation between T_N and \mathcal{M}_s near a QCP is predicted using the corresponding field theory

$$T_N = \sqrt{\frac{12c^3}{5}} \mathcal{M}_s. \quad (3)$$

Notice the original prediction in reference [14] has $c_1 c_2 c_3$ instead of c^3 for anisotropic systems. Here c_i refers to the spinwave velocity in i direction. On the other hand, we use the c defined in previous section to examine the validity of the prediction for an anisotropic system. Interestingly, at first glance it seems that we investigate a modified prediction which is slightly different from the original one determined in reference [14]. However, the analysis performed in our study is in principle equivalent to verifying the original prediction. This can be understood as follows. To calculate the spinwave velocity c_i corresponding to the i direction for each $i \in \{1, 2, 3\}$, one needs to employ a condition in the simulations so that the method used does not favor any particular spatial direction. For the idea we consider here, the most natural requirement is to demand that the square of three spatial winding numbers $\langle W_1^2 \rangle$, $\langle W_2^2 \rangle$, and $\langle W_3^2 \rangle$ take the same value. This condition can be fulfilled by adjusting the aspect ratio of the box sizes used in the simulations. Once this criterion is met, the c_i which corresponds to (the finite box size) L_i is then given by $c_i(L_i) = L_i/\beta$. Here β is the inverse temperature so that each $\langle W_i^2 \rangle$ for $i \in \{1, 2, 3\}$ is equal to the temporal winding number squared $\langle W_t^2 \rangle$. The bulk c_i can be determined by considering the convergence of c_i at box sizes L_i and $2L_i$ for sufficiently large L_i . Notice the original prediction in reference [14] has a factor $c_1 c_2 c_3$. For a finite lattice with volume $L_1 L_2 L_3$ so that the condition of the validity of our method is satisfied, $c_1(L_1) c_2(L_2) c_3(L_3)$ is given by $L_1 L_2 L_3 / \beta^3$ which is exactly the definition of the quantity c^3 introduced here. As a result, the c^3 defined here correctly approaches the bulk $c_1 c_2 c_3$ in the thermodynamics limit. In conclusion, the way we proceed in this investigation is in principle equivalent to examining the

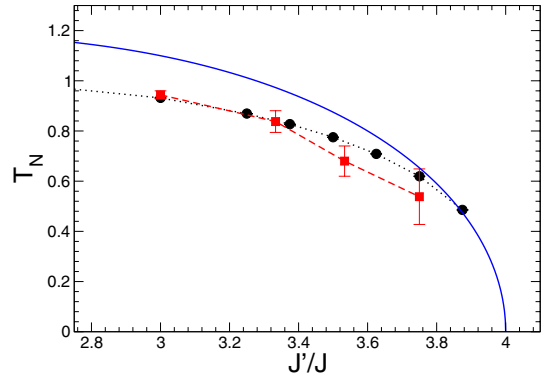


Fig. 5. Results of T_N as a function of J'/J determined by Monte Carlo simulations (solid circles), series expansion (solid squares) as well as field theory calculations (solid curve). The field theory and series expansion results are estimated and reproduced from reference [14]. The dashed and dotted lines are added to guide the eye.

original relation predicted in reference [14]. Notice in real simulations, the condition that the square of three spatial winding numbers take the same value can only be reached approximately due to the discreteness of finite lattices, hence leads to the inequality used above when calculating c with this method. To verify equation (3), in reference [14] the numerical values of T_N , c , and \mathcal{M}_s for various couplings J'/J are determined numerically using the series expansion method. Further, the agreement between the numerical results from series expansion calculations and the field theory prediction is shown to be reasonably good. The quantum Monte Carlo determination of T_N and \mathcal{M}_s for the (3+1)-dimension ladder-dimer model is available in reference [16] as well. Notice that to quantitatively investigate the relation in equation (3), one needs to additionally calculate c . This motivates our study presented here. As a first step to quantitatively study equation (3), in Figure 4 we have already compared our Monte Carlo results for \mathcal{M}_s with those determined by the series expansion method obtained in reference [14]. The consistency of \mathcal{M}_s calculated with these two different methods is impressive. Next, we compare our Monte Carlo data of T_N with the series expansion results available in reference [14]. Such a comparison is presented in Figure 5. Near the QCP $J'/J \sim 0.4$, the consistency between the values of T_N determined by these two different methods is reasonably good as well. Finally, equation (3) implies that the curve of $T_N/\sqrt{c^3}$ as a function of \mathcal{M}_s should be linear assuming the logarithmic correction is not taken into account. In Figure 6 we compute $T_N/\sqrt{c^3}$ as a function of \mathcal{M}_s . Indeed qualitatively the curve shown in Figure 6 is linear in \mathcal{M}_s . A fit of the $T_N/\sqrt{c^3}$ data for $J'/J = 2.5, 3.0, \dots, 3.875$ in Figure 6 to the expression $a + b\mathcal{M}_s$ leads to $a = 0.0117(20)$ which is slightly above the expected value $a = 0$. We attribute such deviation to the logarithmic correction not taken into account in our analysis. Since the obtained $a = 0.0117(20)$ is only slightly above zero, one expects that for the considered parameters J'/J , either the effect due to the logarithmic correction is small or this correction

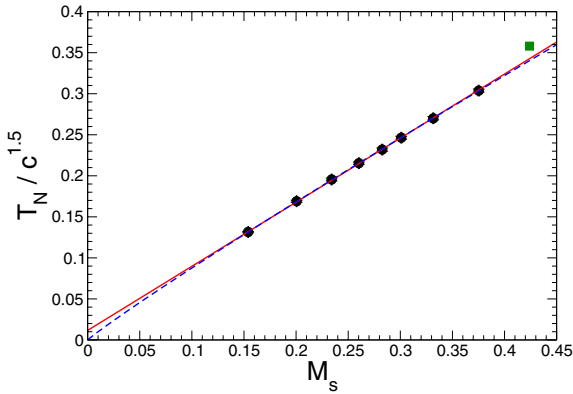


Fig. 6. Monte Carlo data of $T_N/\sqrt{c^3}$ as functions of \mathcal{M}_s . While the solid line is the result of fitting the data to the form $a + b\mathcal{M}_s$, the dashed line is obtained using the ansatz $b_1\mathcal{M}_s + d_1\mathcal{M}_s \log(\mathcal{M}_s)$ for the fit. The square symbol stands for the result associated with $J'/J = 1.0$ and is obtained using the calculations in references [19,20].

only sets in significantly for the region with much stronger spatial anisotropy. Interestingly, the value of b obtained from the fit is about half of the predicted value $\sqrt{12/5}$. Although we have argued that the way we proceed in this study is in principle equivalent to examining the original prediction, one possible explanation for the deviation between the slope extracted here and $\sqrt{12/5}$ is that we use c^3 instead of $c_1c_2c_3$ in equation (3). This needs further investigation. Nevertheless, we do find that equation (3) is valid to a great extent using our definition of c . Without the explicit form of the logarithmic correction, we are not able to properly describe the data in our analysis. On the other hand, in the spirit of the expansion in chiral perturbation theory for Quantum Chromodynamics, it is naturally to include $\mathcal{M}_s \log(\mathcal{M}_s)$ as the additional correction. Remarkably, we can reach a good result using the ansatz $b_1\mathcal{M}_s + d_1\mathcal{M}_s \log(\mathcal{M}_s)$ for the fit (dashed line in Fig. 6). Notice the resulting fitting curves of these two different ansätze match nicely in the regime where our Monte Carlo data are available.

7 Discussions and conclusions

In this report, we have simulated the three-dimensional ladder-dimer quantum Heisenberg model using the first principles Monte Carlo method. Our motivation is to investigate quantitatively the newly established universal relation between T_N and \mathcal{M}_s near a QCP. We find that for all the quantities considered here, such as T_N and \mathcal{M}_s , our Monte Carlo calculations agree nicely with the corresponding results determined by the series expansion method. Assuming equation (3) is correct without considering the correction, then $T_N/\sqrt{c^3}$ as a function of \mathcal{M}_s should vanish at $\mathcal{M}_s = 0$. We find that the deviation between the extrapolated result of $T_N/\sqrt{c^3}$ and zero is of the order 10^{-2} . This implies that either the logarithmic correction is small or this correction only sets in significantly

for the region with much stronger spatial anisotropy. Indeed, our Monte Carlo data of $T_N/\sqrt{c^3}$ can be described well by an empirical ansatz $b_1\mathcal{M}_s + d_1\mathcal{M}_s \log(\mathcal{M}_s)$. Further, the resulting fitting curves of the two different ansätze used in our analysis match nicely in the regime where our Monte Carlo data are available. This confirms that indeed the logarithmic correction only sets in significantly for the region beyond what we have studied. Finally, using the spinwave theory and series expansion results available in references [19,20], one obtains $T_N \sim 0.944$, $\mathcal{M}_s \sim 0.424$, and $c \sim 1.9091J$ for the isotropic case $J'/J = 1.0$. The data point of $T_N/\sqrt{c^3}$ and its corresponding \mathcal{M}_s for $J'/J = 1.0$ is depicted as the square in Figure 6. It is remarkable that the prediction equation (3) is valid (qualitatively) all the way up to $\mathcal{M}_s \sim 0.4$.

Partial support from NSC and NCTS (North) of R.O.C. is acknowledged. We appreciate greatly useful discussions with A.W. Sandvik and U.-J. Wiese.

References

1. V. Hinkov, P. Bourges, S. Pailhes, Y. Sidis, A. Ivanov, C.D. Frost, T.G. Perring, C.T. Lin, D.P. Chen, B. Keimer, *Nat. Phys.* **3**, 780 (2007)
2. V. Hinkov et al., *Science* **319**, 597 (2008)
3. T. Pardini, R.R.P. Singh, A. Katanin, O.P. Sushkov, *Phys. Rev. B* **78**, 024439 (2008)
4. S. Sachdev, C. Buragohain, M. Vojta, *Science* **286**, 2479 (1999)
5. M. Vojta, C. Buragohain, S. Sachdev, *Phys. Rev. B* **61**, 15152 (2000)
6. S. Sachdev, M. Troyer, M. Vojta, *Phys. Rev. Lett.* **86**, 2617 (2001)
7. M. Troyer, *Prog. Theor. Phys. Supp.* **145**, 326 (2002)
8. Munehisa Matsumoto, Chitoshi Yasuda, Syngge Todo, Hajime Takayama, *Phys. Rev. B* **65**, 014407 (2002)
9. K.H. Höglund, A.W. Sandvik, *Phys. Rev. Lett.* **91**, 077204 (2003)
10. L. Wang, K.S.D. Beach, A.W. Sandvik, *Phys. Rev. B* **73**, 014431 (2006)
11. Kwai-Kong Ng, T.K. Lee, *Phys. Rev. Lett.* **97**, 127204 (2006)
12. A.F. Albuquerque, M. Troyer, J. Oitmaa, *Phys. Rev. B* **78**, 132402 (2008)
13. Y. Kulik, O.P. Sushkov, *Phys. Rev. B* **84**, 134418 (2011)
14. J. Oitmaa, Y. Kulik, O.P. Sushkov, *Phys. Rev. B* **85**, 144431 (2012)
15. Ch. Rüegg et al., *Phys. Rev. Lett.* **100**, 205701 (2008)
16. S. Jin, A.W. Sandvik, *Phys. Rev. B* **85**, 020409(R) (2012)
17. A.W. Sandvik, *Phys. Rev. B* **66**, R14157 (1999)
18. O. Nohadani, S. Wessel, S. Haas, *Phys. Rev. B* **72**, 024440 (2005)
19. J. Oitmaa, C.J. Hamer, Zheng Weihong, *Phys. Rev. B* **50**, 3877 (1994)
20. J. Oitmaa, Weihong Zheng, *J. Phys.: Condens. Matter* **16**, 8653 (2004)